

Contents lists available at ScienceDirect

# Acta Biomaterialia

journal homepage: www.elsevier.com/locate/actbio



Full length article

# Adhesive contact and protein elastic modulus tune orb weaving spider glue droplet biomechanics to habitat humidity



Brent D. Opell\*, Hannah Mae Elmore, Mary L. Hendricks

Department of Biological Sciences, Virginia Tech, Blacksburg, VA 24061, USA

#### ARTICLE INFO

Article history:
Received 26 March 2022
Revised 2 August 2022
Accepted 8 August 2022
Available online 13 August 2022

Keywords: Bioadhesive Biomechanics Environmental responsiveness Soft matter

#### ABSTRACT

Tiny glue droplets along the viscous capture threads of spider orb webs prevent insects from escaping. Each droplet is formed of a protein core surrounded by a hygroscopic aqueous layer, which cause the droplet's adhesion to change with humidity. As an insect struggles to escape the web, a thread's viscoelastic core proteins extend, transferring adhesive forces to the thread's support fibers. Maximum adhesive force is achieved when absorbed atmospheric moisture allows a flattened droplet to establish sufficient adhesive contact while maintaining the core protein cohesion necessary for force transfer. We examined the relationship between these droplet properties and adhesive force and the work of extending droplets at five relative humidities in twelve species that occupy habitats which have different humidities. A regression analysis that included both flattened droplet area and core protein elastic modulus described droplet adhesion, but the model was degraded when core protein area was substituted for droplet. Species from low humidity habitats expressed greater adhesion at lower humidities, whereas species from high humidity habitats expressed greater adhesion at high humidities. Our results suggest a general model of droplet adhesion with two adhesion peaks, one for low humidity species, which occurs when increasing droplet area and decreasing protein cohesion intersect, and another for high humidity species, which occurs when area and cohesion have diverged maximally. These dual peaks in adhesive force explain why some species from intermediate and high humidity habitats express high adhesion at several humidities.

### Statement of significance

We characterized the effect of humidity on the adhesion of twelve orb weaving spider species' glue droplets and showed how humidity-mediated changes in the contact area of a droplet's outer, hygroscopic aqueous layer and the stiffness of its protein core affect droplet performance. This revealed how droplet adhesion has been tuned to the humidity of a species' habitat and allowed us to revise a model that describes the environmental determinants of droplet biomechanics.

© 2022 The Authors. Published by Elsevier Ltd on behalf of Acta Materialia Inc.

This is an open access article under the CC BY-NC-ND license (http://creativecommons.org/licenses/by-nc-nd/4.0/)

### 1. Introduction

Spider viscous prey capture thread (Fig. 1A) is among the most widely used animal bioadhesives, being employed by 4706 species of orb weaving spiders (in order of decreasing number of species, members of the families Araneidae, Tetragnathidae, Anapidae, Mysmenidae, Theridiosomatidae, Symphytognathidae, and Synaphridae), 2819 species of cobweb spiders (Theridiidae and Nestici-

\* Corresponding author.

E-mail address: bopell@vt.edu (B.D. Opell).

dae), and at least some of the 4718 species of sheet web spiders (Linyphiidae) [3]. In contrast with 1600 species of nonparasitic barnacles [4] and 484 species of marine mussels [5] that attach to rocks with adhesives that stiffen after being secreted [6,7], orb spider glue droplets remain pliable, being hydrated by a hygroscopic solution that surrounds a droplet's denser protein core (Fig. 1B). These core proteins have been termed glycoproteins, although phosphorylated proteins have also been identified in droplet cores [8]. As an insect struggles to escape from a web, each droplet extends and transfers its adhesive force to the thread's supporting flagelliform fibers in suspension bridge fashion (Fig. 1B and C) [9–12]. The biomechanical efficiency of this adhesive

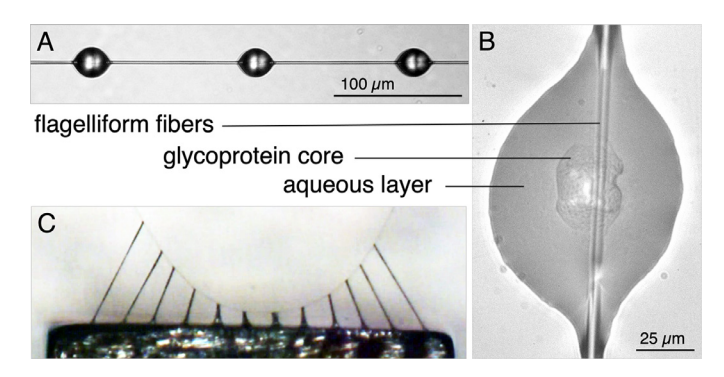


**Fig. 1.** Viscous prey capture thread. A. Capture thread of *Verrucosa arenata*. B. Flattened glue droplet of *V. arenata*. C. *Argiope trifasciata* thread assuming a suspension bridge configuration as it is pulled from a 2 mm wide surface.

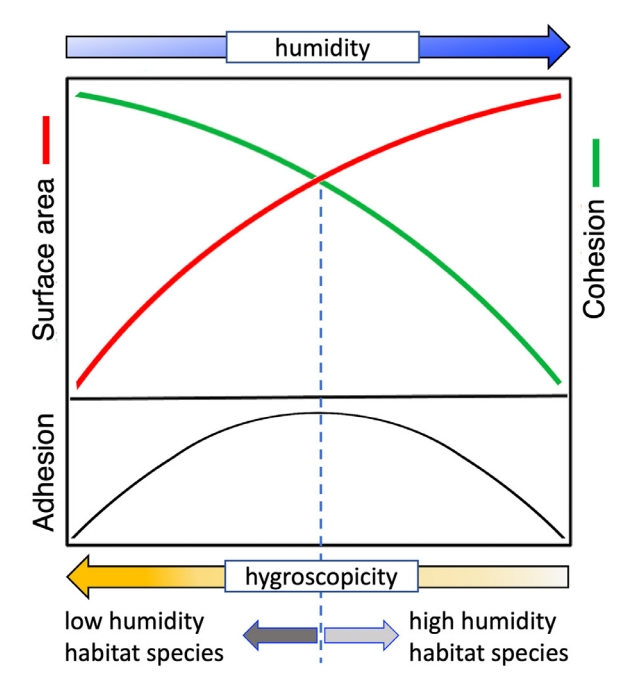


**Fig. 2.** Model of orb web spider glue droplet adhesive force as modified from Amarpuri et al. [1]. As humidity increases a hygroscopic droplet absorbs water, causing its adhesive protein to soften, its surface area of contact to increase and its cohesion to decrease. When optimal surface area and cohesion are established, maximum adhesive force is expressed. In species that occupy low humidity habits and have more hygroscopic droplets, this balance is achieved at lower humidities, whereas species adapted to high humidity habitats express maximum adhesive force at higher humidities.

system relies on the scaling of flagelliform fiber and core protein stiffness, with core protein elastic modulus being, on average, one sixth that of flagelliform fiber elastic modulus [13].

Our understanding of how this adhesive system performs has been guided by a model that attributes maximum glue droplet adhesion to an optimal balance of adhesive contact area and adhesive cohesion (referred to in other studies as surface dissipation and bulk dissipation, respectively) [1,14], which ensures sufficient initial adhesion while maintaining the core protein's ability to transfer force to support fibers (Fig. 2) [1]. In this study we examined this model by constructing, matched droplet property and force plots for the glue droplets of twelve orb weaving species. As the hygroscopicity of orb web glue droplets differ among species [2,15,16], we included species that are found in different habitats: on exposed vegetation, along forest edges, within humid forests, and near water; as well as species that are nocturnal (Fig. 3). This also allowed us to test another hypothesis that has guided research

on orb web capture threads: The more hygroscopic glue droplets of species that live in dryer habitats and experience lower humidity when they forage ensure that these species' adhesive proteins remain hydrated and express maximum adhesive force at lower humidity. In contrast, species found in more humid environments have less hygroscopic droplets, which prevents their proteins from becoming oversaturated with water and allows them to achieve maximum adhesion at higher humidity (Fig. 2) [1,2,17]. Support for this hypothesis comes from observations that glue droplet viscosity, thread adhesion, and protein elastic modulus values are very similar when measured at each species' foraging humidity, despite these values differing greatly across humidities [1,2,18].

Viscous capture threads are complex, self-assembling strands, whose flagelliform fibers and protein cores are both products of spidroin genes [8,19–22]. Capture threads form when a flagelliform fiber emerges from a spigot on each of a spider's paired posterior lateral spinnerets. As it emerges, this fiber is coated with an aqueous solution from two flanking aggregate glands [23]. After the coated fibers from the two spinnerets merge, Rayleigh-Plateau instability quickly reconfigures the aggregate cylinder into droplets [24]. A protein core condenses within each droplet, leaving an aqueous layer that covers both this core and the flagel-liform fibers within and between droplets (Fig. 1A and B). Inorganic salts, low molecular mass compounds (LMMCs), and amorphous proteins that remain in the aqueous layer confer droplet hygroscopicity, hydrate and condition the protein core, and maintain flagelliform fiber extensibility [15,16,18,25–28].

A small cylindrical region termed a granule lies at the center of a droplet's protein core and is assumed to anchor the protein to flagelliform fibers [29]. Granules are most easily seen with transmitted light and, therefore, are not usually visible with epiillumination, which we used in this study (Fig. 1B). It is not known if a granule is formed of proteins that are distinct from others in the droplet's core or if this region represents a configurational change in core proteins that contact flagelliform fibers. However, this junction is very robust and is usually maintained through 40 droplet adhesion, extension, and pull-off cycles [30]. Although not visible under a standard light microscope, amorphous protein in the aqueous layer can be detected with spectroscopy and with optical and confocal Raman microscopy [25] although X-ray scattering distinguishes only flagelliform fibers from other droplet constituents [31]. Because glycoprotein is a known biological adhesive, a droplet's protein core had been assumed to be its glue until these amorphous proteins were discovered and shown to also be adhe-

The LMMCs in the aqueous layer not only confer droplet hygroscopicity, but they also solvate core protein, making it more adhesive [27]. This may ensure that core proteins combine with amorphous proteins, which have established initial surface adhesion, to produce a secure surface bond that is able to withstand force that is generated as a droplet extends. However, it is not clear if total droplet surface area or core protein surface area alone limits a droplet's adhesion. Droplet area would greatly increase adhesive contact (Fig. 1B), but would require the more diffuse amorphous proteins to transfer a large percentage of their adhesive force to core proteins, which confer strength to an extending droplet filament (Fig. 1C). Therefore, we examined the effects on droplet adhesion of both total droplet surface area and of core protein surface area in combination with core protein cohesion to determine which scenario best described droplet performance.

As humidity increases, a droplet's aqueous layer attracts atmospheric water, some of which is incorporated into the protein core, plasticizing this material and allowing it to more easily extend [32]. Cohesion describes the strength of intermolecular forces that hold a material together, although measuring this force in soft materials like gels is challenging [33]. Elastic (Young's) mod-

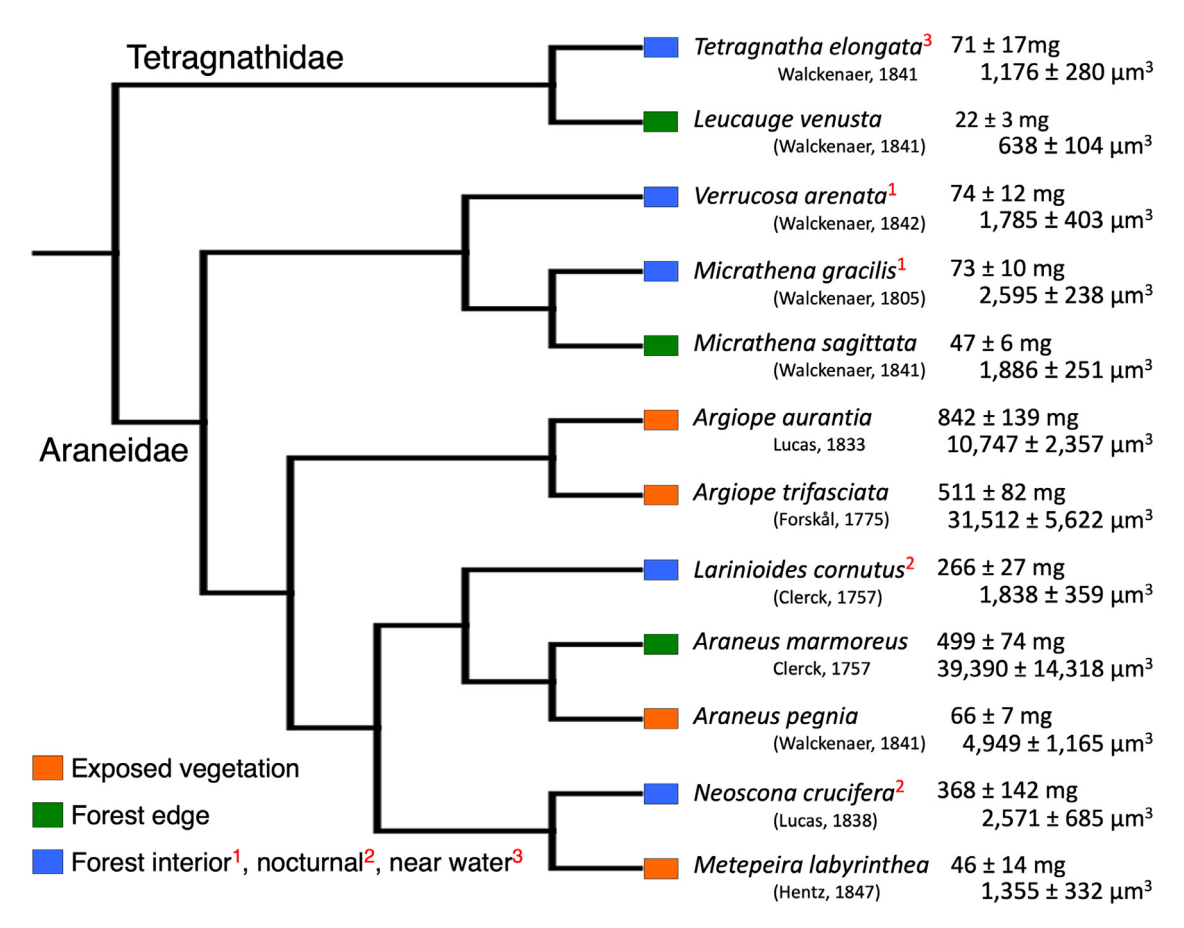


Fig. 3. Study species and their humidity habitat assignments from Opell et al. [2]. Mean and standard error of adult female mass shows the size range species that were studied and mean and standard error of droplet core protein volumes at 55% relative humidity shows the range in size of this droplet component.

ulus describes the volume-specific energy required to extend a material during its elastic phase. As cohesion must be overcome for a droplet's protein core to extend, elastic modulus serves as a volume-specific index of protein cohesion. In principle, the reciprocal of extension length per core protein volume would also be an appropriate index of cohesion. However, in species that are found in low and intermediate humidity habitats, maximum droplet extension is achieved at low and intermediate humidity and decreases thereafter because a droplet's protein core becomes oversaturated with water and is more easily pulled from a surface (Figs. 2 and 5 in [2]). For these species, this index of cohesion would first decrease and then increase as humidity increased. We draw on our recent study, which characterized the elastic modulus of the twelve species that are included in the current study at 20, 37, 55, 72, and 90% (RH), as well as on unreported flattened droplet and core protein surface area values and forces of droplets at pull-off from that study [2].

### 2. Materials and methods

# 2.1. Collecting threads and preparing droplets for testing and establishing test conditions

We review the methods used in our previous study, which addresses additional technical considerations associated with characterizing the properties and performance of orb spider glue droplets [2]. All web samples were collected from orb webs constructed in the field to ensure that spiders experienced natural conditions and feeding regimes. Samples of the nocturnal species *Neoscona cru*-

cifera and Larinioides cornutus were collected in the early evening and samples of the other ten species in the early morning soon after they were constructed. All tests of threads from nocturnal species were completed by 16:00 on the day following their collection and tests of the other species' threads by 16:00 on the day they were collected. We used aluminum rings and frames with double sided tape on their rims to collected sectors of orb webs constructed by 12 - 14 adult female spiders of each study species. To prevent threads from being damaged or contamination by dust and pollen, these samples were placed in a closed box and stored in the laboratory at approximately 23°C and 50% RH until they were prepared for study. In the laboratory we transferred threads from each sample to the raised supports of microscope slide samplers [34]. Double sided tape on the forceps used to transfer threads and on the web sampler's supports ensured that the native tensions of these 4800 µm thread spans were maintained.

Suspended and flattened droplets were photographed and droplet extension movies captured while threads were enclosed in a glass-covered aluminum chamber that rested on the stage of a Mitutoyo FS60 inspection microscope. Temperature was maintained at 23°C by a thermostat-controlled Peltier thermoelectric module attached to the chamber wall. During tests we continually monitored chamber humidity with a Fisher Scientific® Instant Digital Hygrometer, whose probe tip extended through the chamber wall. Test humidities of 20, 37, 55, 72, and 90% RH were established and maintained during tests using silica gel desiccant beads to lower humidity and distilled water saturated Kimwipes® to raise humidity. Small adjustments were made by either drawing

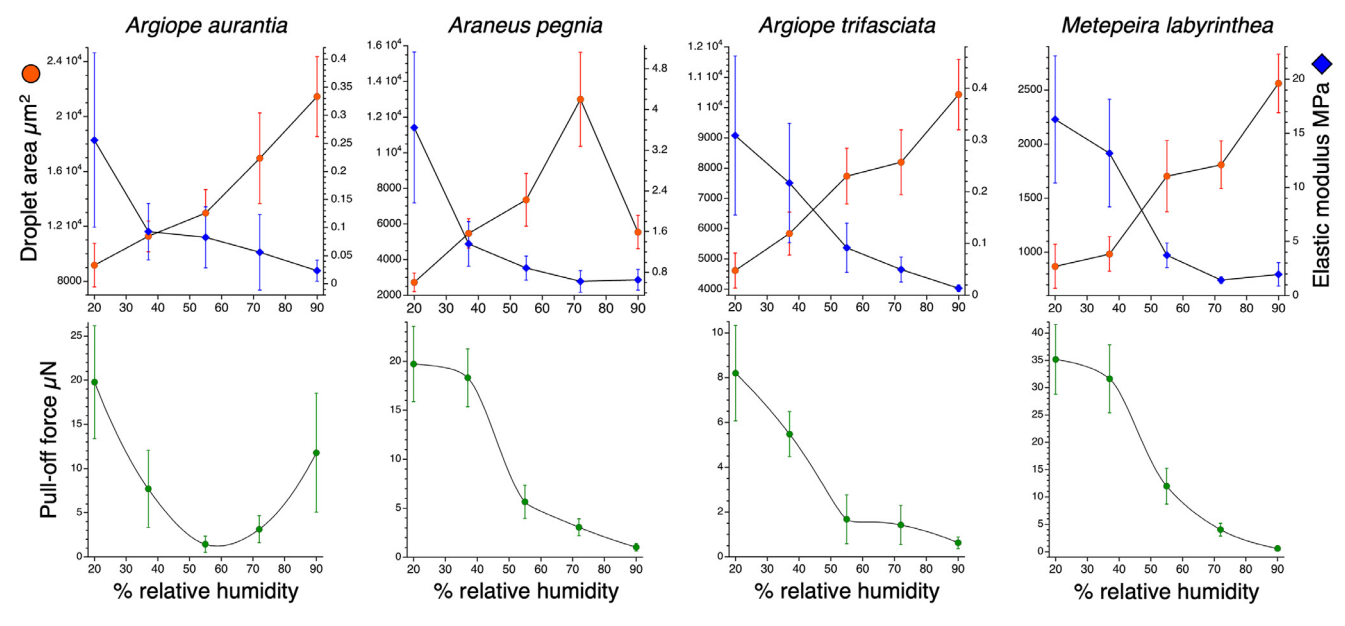


Fig. 4. Matched droplet area, elastic modulus, and pull-off force values of the four low humidity species that build webs on exposed vegetation. Lines connecting points are interpolations of these values. Error bars are  $\pm$  1 standard error.

room air into the chamber or gently blowing humid air into the chamber to raise humidity through a tube connected to a port in the side of the chamber. A droplet remained at a test humidity for about 6–8 min before being photographed, flattened, or extended.

### 2.2. Flattening and extending droplets

Three glue droplets were photographed and then flatten to reveal their protein cores. This was done by dropping a glass cover slip onto the suspended thread from a magnetically tripped device contained with the chamber. To ensure consistent flattening, we then pressed the cover slip against the thread supports of the microscope slide sampler with a small steel probe that was inserted into the chamber through a port. The same three droplets were photographed again within about 30 s after being flattened (Fig. 1B). The total surface area and core protein surface area of each droplet was measured and their mean values used as an individual's value. We divided a droplet's suspended volume by its flattened area to determine its thickness. We determined core protein volume, which is necessary for computing protein elastic modulus, by multiplying protein surface area by droplet thickness.

We prepared two additional thread samples per individual for droplet extension tests by isolating a glue droplet at the center each 4800  $\mu m$  span. This ensured that the tip of a probe used to extend droplets contacted only a single droplet. We extended each isolate droplet by contacting it with the tip of a cleaned, polished steel probe, pressing the thread 500  $\mu m$  into the probe to ensure droplet adhesion, and, within about 15 s, engaging a stepping motor connected to the microscope stage's X-axis, which withdrew the thread from the probe at a constant velocity of 69.6  $\mu m$  s<sup>-1</sup>. A 60 frames-per-second movie recorded the droplet's extension.

Close examination of extension movies showed that at all humidities nearly all droplets pulled cleanly from the probe, leaving no visible protein residue. This is consistent with findings that a short glue droplet contact period similar to ours resulted in complete adhesive peeling and clean droplet release [14]. At higher humidities, the glue droplets of some species found in low humidity habitats transitioned from what has been termed phase 1 extension, which is characterized by an extending protein filament being

completely surrounded by aqueous material, as it is during normal suspension bridge formation (Fig. 1C), to phase 2 extension, which begins when tiny aqueous material droplets form on the protein filament, exposing portions of the filament to the drying effects of air [35]. In these cases, we equated the end of phase 1 extension with droplet pull-off and, for simplicity, refer to both terminal designations as droplet pull-off.

# 2.3. Analyzing droplet extension movies and determining elastic modulus and force

When analyzing a droplet extension movie, we used the angular deflection of the thread span that supported a droplet to compute the force on the droplet at the initiation of extension and at each 20% extension interval to pull-off. As descried more fully in previous studies [2,35-37], determining the force on a droplet involved the following steps: 1. The deflection angle was used to compute the elongation of the initially 2400 µm long support line on each side of a droplet, 2. The force on each half of the support line was computed from the line's extension and the diameters and elastic modulus of the line's flagelliform fibers, and 3. These force vectors were summed and resolved to determine the force on the extending droplet. Dividing this force by the cross-sectional area of the protein filament at a given extension length, which was determined by dividing core protein volume by droplet length, yielded the true stress on the protein filament. We determined the corresponding true strain on a droplet filament as the natural log of (difference between the filament's length and the initial the diameter of the droplet's protein core) divided by core protein diameter. Elastic modulus was then computed as the slope of the linear elastic phase of each species' humidity-specific true stress-strain curve.

An issue that we confronted in our previous study, and one that effects the current study, is that the elastic modulus of a thread's flagelliform fibers had been determined in the range of 50% (typical laboratory) RH [38]. Although flagelliform fibers remain covered by an aqueous layer, it is possible and perhaps likely that the water content of this layer, which changes in ambient humidity, causes flagelliform fibers to lose water and stiffen at lower humidities and gain water and become more extensible at higher humidities. If

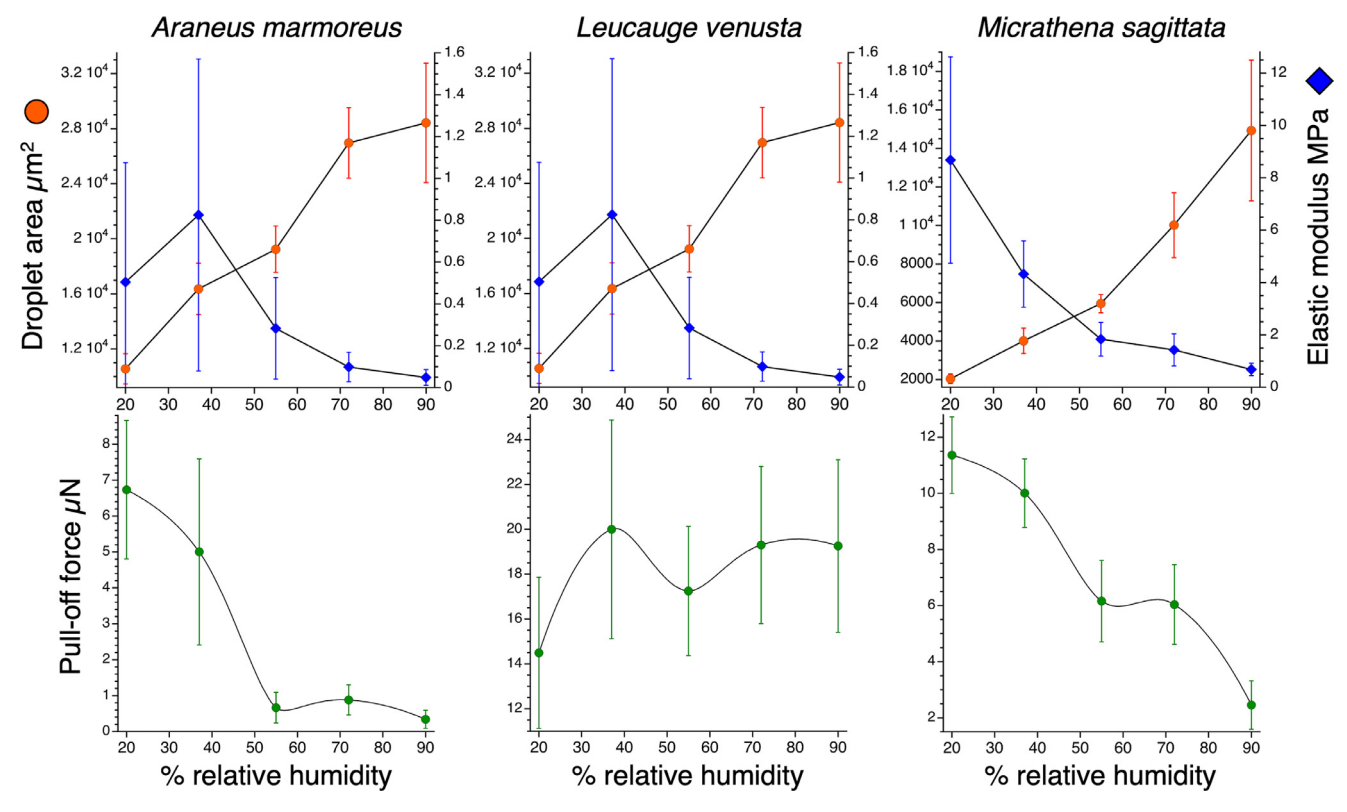


Fig. 5. Matched droplet area, elastic modulus, and pull-off force values of the three intermediate humidity species that build webs on forest edge vegetation. Lines connecting points are interpolations of these values. Error bars are  $\pm$  1 standard error.

this occurs, more force would be required to achieve the same support line deflection at lower humidities than at higher humidities. We addressed this in our previous study by progressively increase protein elastic modulus values at 37 and 20% RH and progressively decrease values at 72% and 90% RH, using droplet extension per protein core volume as an index of the degree of humidity-induced protein softening.

Lacking a comparable index to use in this study to account for the effect of humidity on the elastic modulus of flagelliform fibers whose deflection we used to compute the force on a droplet at pull-off, as taken from the literature for ten species [39] and newly measured for A. pegnia and M. sagittata [37], we increased the measured elastic modulus of each species' fibers by 5% at 37% RH and 10% at 20% RH and reduced their values by 5% at 72% RH and 10% at 90% RH. The effects of these adjustments on the computed forces on droplets at pull-off can be seen by comparing unadjusted and adjusted values (respectively) of M. sagittata: 20% RH 10.33 and 11.36 μN, 37% RH 10.10 and 10.60 μN, unchanged 55% RH 6.16  $\mu$ N, 72% RH 6.35 and 6.03  $\mu$ N, 90% RH 2.72 and 2.45  $\mu$ N. We determined the work of extending a droplet to pull-off from the area under its µN force and µm extension curve, computed as the sum of the areas of rectangles defined by the change of length during each 20% extension interval and the mean force on a droplet at the beginning and end of this extension interval. As a droplet was under tension when it began to extend, we subtracted from this total area the area of a narrow rectangle defined by the force on a droplet at the initiation of extension and a droplet's extension length at pull-off.

### 2.4. Assembling and analyzing data

We assembled and analyzed data with JMP (SAS Institute, Cary, N.C.). As most *N. crucifera* droplets were too stiff to adhere at

20% RH, no values are reported for this species at this humidity. The mean elastic modulus values reported in our previous study [2] were computed after outlying values were excluded. In the current study elastic modulus and all other values are from our full, integrated data set, with each individual spider's values being represented at all five test humidities, except, as noted above, for *N. crucifera* at 20% RH.

We used contingency statistics to test the hypothesis that maximum adhesive force and work of droplet extension is expressed at a species' foraging humidity, considering  $P \leq 0.05$  as significant in all comparisons. In these tests we used a 3-humidity ranking scheme by assigned ranks 1, 2, and 3 to exposed vegetation, forest edge, and high humidity (forest interior, nocturnal, and near water) habitats, respectively. To acknowledges that the two nocturnal species forage at high humidity during the night and also at lower humidity during the following day, we also used a 4-humidity ranking scheme that placed the two nocturnal species between the three forest edge species and the three species found in forest interior or near water.

### 3. Results

3.1. The contributions of core protein area and droplet surface area to adhesive force

The following regression model that fitted the twelve species' mean 37, 55, 72, and 90% RH adhesive forces in  $\mu$ N to their mean droplet areas (DA) in  $\mu$ m<sup>2</sup>, protein elastic modulus values (EM) in MPa, and the interaction of droplet area and elastic modulus was highly significant (P < 0.0001, adjusted  $R^2 = 0.77$ ). Each component contributed significantly to the model (P < 0.0001) and the LogWorth and False discovery LogWorth values of droplet area, elastic modulus, and interaction term exceeded the 2.0 cut-off level

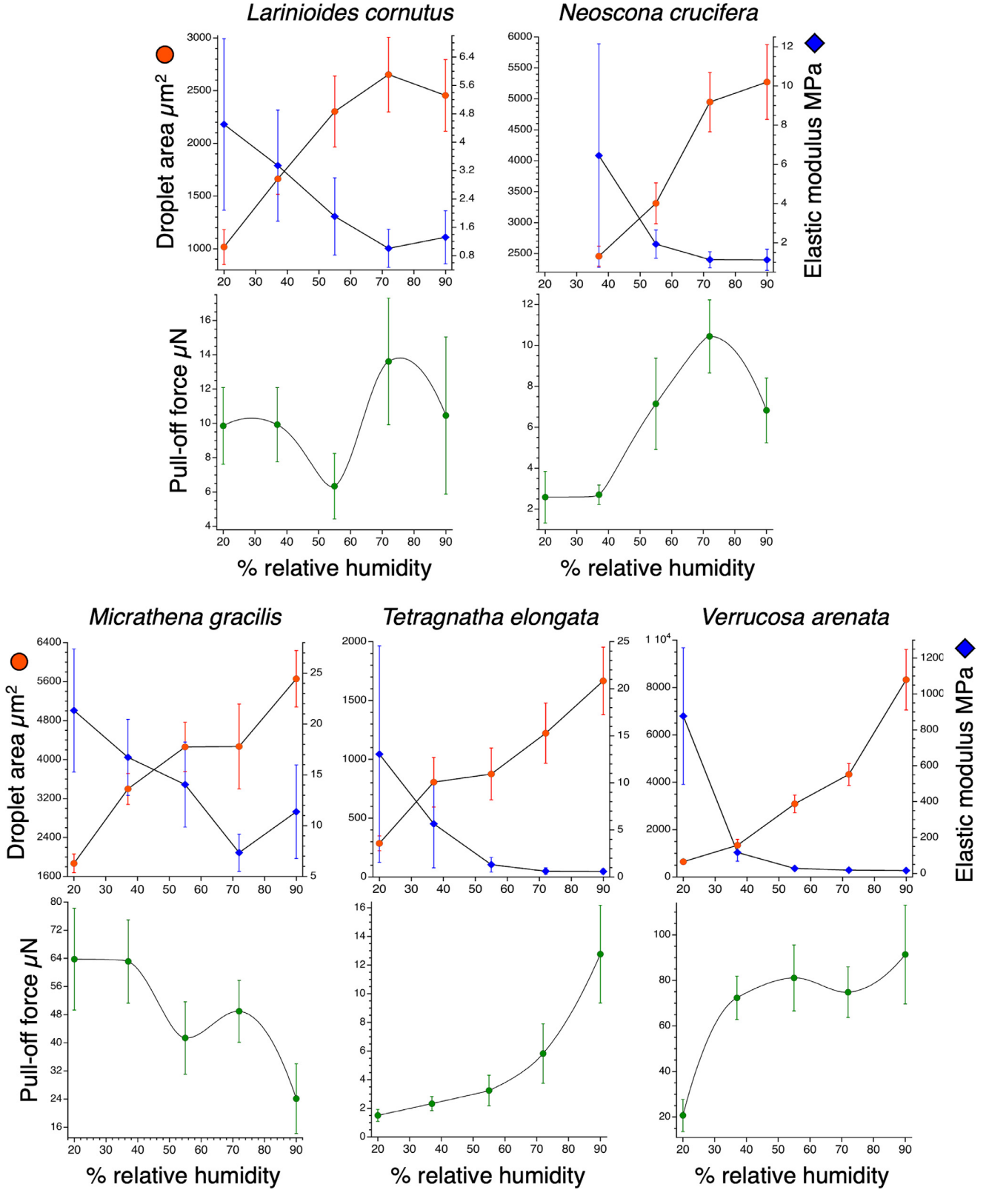


**Fig. 6.** Matched droplet area, elastic modulus, and pull-off force values of the five high humidity species. Larinioides cornutus and N. crucifera are nocturnal, M. gracilis and V. arenata are found in humid forests, and T. elongata is found near water. Lines connecting points are interpolations of these values. Error bars are  $\pm$  1 standard error.

for significant contributions (17.269, 17.269; 18.467, 18.249; and 18.425, 18.249, respectively).

$$AF = ((DA \times 0.01684) + (EM \times 4.4728) + ((EM - 21.7354) \times (DA - 6205.26)) \times 0.0008)) - 97.8071$$
(1)

In contrast, when core protein surface area in  $\mu$ m<sup>2</sup> was substituted for droplet area the model's fitness decreases greatly, having P=0.0006 and adjusted  $R^2=0.23$ . LogWorth and False discovery LogWorth values of core protein area, elastic modulus, and interaction term hovered around 2.0 (1.999, 1.999; 2.305, 2.120; and 2.296, 2.120, respectively).

# 3.2. The relationship of droplet area and protein elastic modulus to adhesive force

We include 20% RH values from plots of droplet area, protein elastic modulus, and adhesive force (Figs. 4-6), but regard these values as reference value that describe droplets at close to their stiffest state and not values that are typically expressed in nature. This is confirmed by field recordings made in habitats where the study species were found showing that 20% RH is much lower than experienced by any of the study species (Fig. 4 in [2]). The four species that are found in exposed, low-humidity habitats exhibited maximum adhesive force at 37% RH or, in the case of A. aurantia, first did so at 37% RH (Fig. 4). Argiope arenata and A. pegnia expressed maximum pull-off force when area and elastic modulus lines crossed and A. trifasciata and M. labyrinthea did so before this occurred, with their lines crossing around 45% RH.The three forest edge species also exhibited adhesive force peaks at 37% RH, which occurred before their area and elastic modulus lines crossed around 45% RH (Fig. 5). However, L. venusta force reached a second force plateau from 70% to 90% RH when their area and elastic modulus lines had greatly diverged and M. sagittata showed a much lower force plateau between 55% and 72% RN.

The five species that occupy high humidity habitats exhibited the widest range of associations between droplet properties and force (Fig. 6). Droplets of the two nocturnal species, L. cornutus and N. crucifera, exhibited maximum pull off force at 72% RH, where droplet area and elastic modulus had diverged, although L. cornutus showed a lower force peak at 37% RH where area and elastic modulus lines crossed. The forest species, M. gracilis and V. arenata, each exhibit two pull-off force peaks. Micrathena gracilis shows a higher peak at 37% RH before area and elastic modulus curves intersect and a lower peak at 72% RH after area and elastic modulus have diverged. Verrucosa arenata exhibits two similar force peaks, one at 55% RH and another at 90% RH, both after area and elastic modulus values have diverged. Droplets of T. elongata, which is found near water, exhibit increasing pull-off force as humidity increases and area and elastic modulus diverges, reaching a maximum value at 90% RH.

# 3.3. Relative contributions of protein area and elastic modulus to adhesive force

Our methods did not allow us to experimentally uncouple the effect of humidity on droplet area and cohesion in ways that would change one value independent of the other as another study has done [14]. To better understand the interaction between these variables, we used regression formula 1 described in Section 3.1 to simulate the effects of enhanced core protein elastic modulus and droplet area on pull-off force (Fig. 7). In these simulations we used humidity-specific mean elastic modulus and area values for species from low, intermediate, and high humidity habitats and expressed modeled pull-off forces as precents of those determined

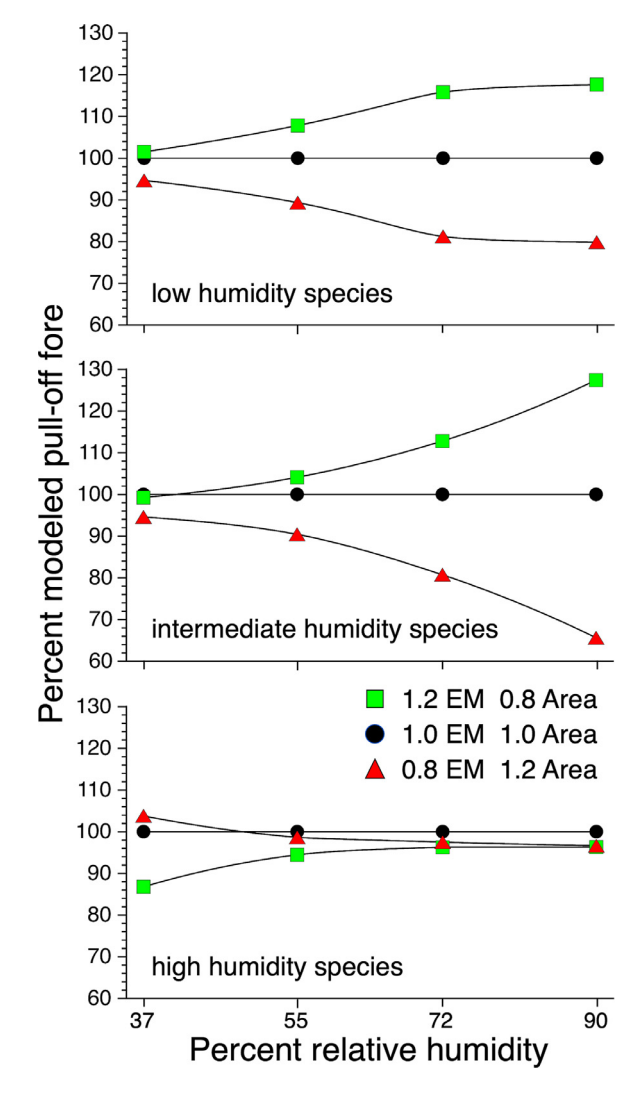


**Fig. 7.** Model of the effects of increased droplet surface area (Area) and elastic modulus (EM) on adhesive force for species in each of the three habitat humidity groups identified in Fig. 3. Pull-off forces were computed from the mean values of species in each group using regression Eq. (1) and are expressed as percent's of the force computed from unaltered values (1.0 EM 1.0 Area).

for each group's unaltered elastic modulus and area values (1.0 EM 1.0 Area). As elastic modulus and area respond inversely to increasing relative humidity (Figs. 4–6), we compared increased elastic modulus and decreased area (1.2 EM 0.8 Area) and decreased elastic modulus and increased area (0.8 EM 1.2 Area). In low and intermediate humidity species enhanced elastic modulus increased pull-off force and enhanced area decreased pull-off force. These changes in pull-off force were greater and more continual in intermediate humidity species, with pull-off force plateauing at 72% RH in low humidity species. These simulations had much less effect on the modeled forces of high humidity species. At 37% RH increased elastic modulus reduced pull-off force while increased area resulted in a small increase in pull-off force. At relative humidities of 55% and greater changing either elastic modulus or area caused small decreases in pull-off force.

### 3.4. Performance of regression model of adhesive force

A comparison of measured adhesive force and that computed with regression Eq. (1) shows the limits of this model in describing adhesive force across species (Fig. 8). Good correspondence be-

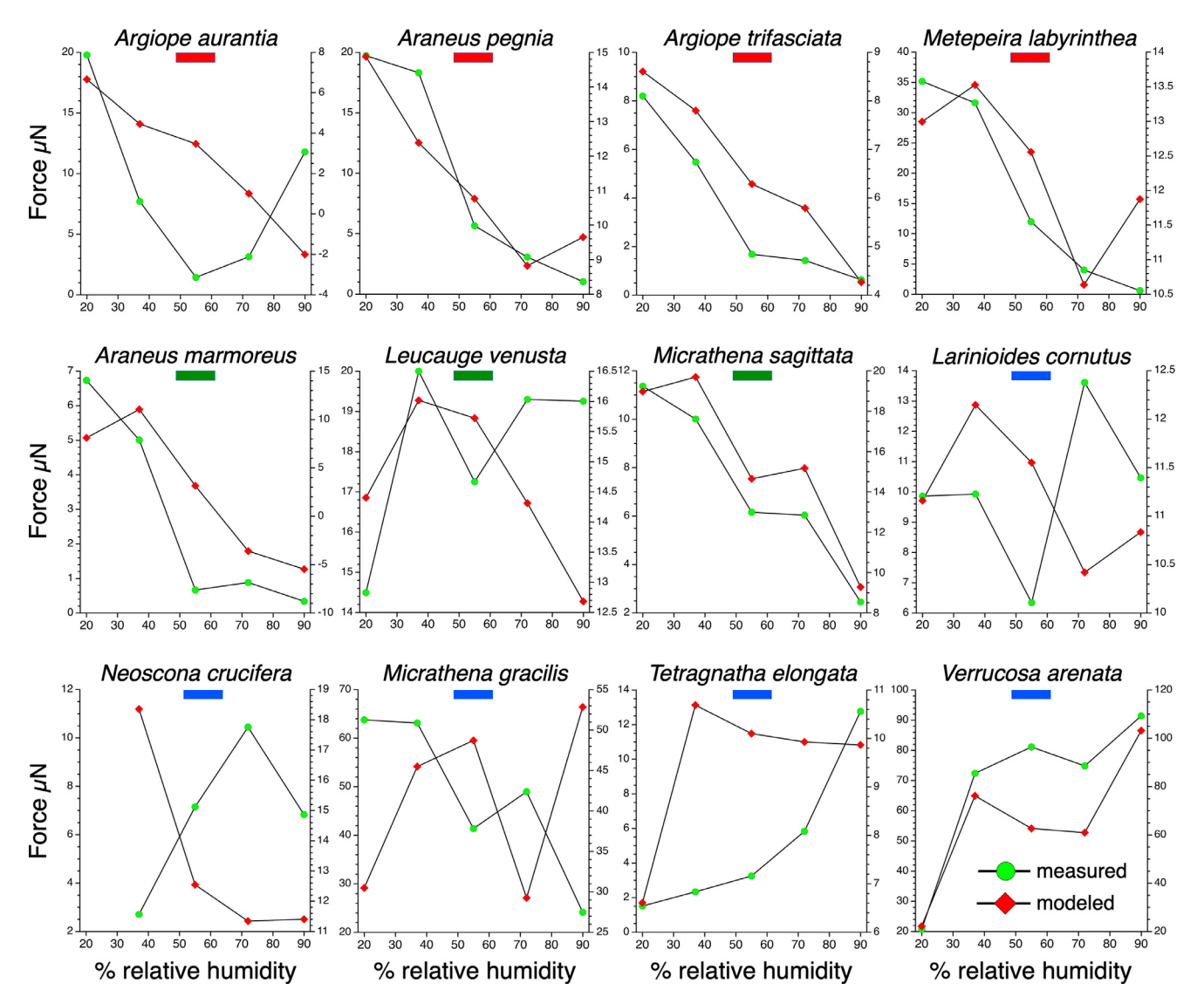


Fig. 8. Comparison of measured adhesive force and force modeled from droplet surface area and core protein elastic modulus using regression Eq. (1). Color bars denote the species' foraging humidity: red = low, green = intermediate, blue = high.

tween measured and modeled forces was observed in six species, which represented all three habitat humidity groups: *A. pegnia, A. trifasciata, M. labyrinthea, A. marmoreus, M. sagittata,* and *V. arenata.* The model performed poorly for four of the five high humidity species, *L. cornutus* and *M. gracilis,* whose pull-off forces oscillated across humidities, and for *N. crucifera* and *T. elongata,* where pull-off force increased continually from 35% RH to 72% RH and 90% RH, respectively. This may be due to the general regression model's insensitivity to changes in core protein elastic modulus and droplet area (Fig. 7).

Separate regression models for species from low and intermediate humidity habitats were not significant. Low humidity species had droplet area, core protein elastic modulus, and interaction terms LogWorth values between 0.550 and 0.895 and intermediate humidity species between 1.518 and 1.938. However, the regression model for the five high humidity species' adhesive forces (AF) provided below was highly significant (P < 0.0001, adjusted  $R^2 = 0.79$ ), with droplet area (DA) in  $\mu$ m², core protein elastic modulus (EM) in MPa, and the interaction of these two variables each having P < 0.0001, LogWorth values of 7.952, 7.029, and 6.963 and False discovery LogWorth values of 7.475, 6.963, and

6.963, respectively.

$$AF = ((DA x 0.04073) + (EM x 1.95178) + ((EM - 48.723) x (DA - 2838.28)) x 0.00089)) - 108.891$$
(2)

However, pull-off forces of the five high humidity species computed with this formula neither differ from those computed with comprehensive formula 1 (P < 0.0001, r = 0.99) nor correspond more closely with measured values than those computed with the comprehensive formula (P < 0.0001, r = 0.80 vs P < 0.0001, r = 0.83).

### 3.5. Habitat humidity and maximum adhesive force

The adhesive forces of eight species (*A. aurantia, A. pegnia, A. trifasciata, L. cornutus, M. labyrinthea, M. sagittata, N. crucifera, T. elongata*) peaked at a single post-20% RH. The humidity at which each of these species exhibited maximum force was ranked 1 to 4, corresponding to humidities 37%, 55%, 72%, and 90% RH, respectively. Contingency tests showed that habitat humidity rankings and maximum force rankings were correlated for both the 3-

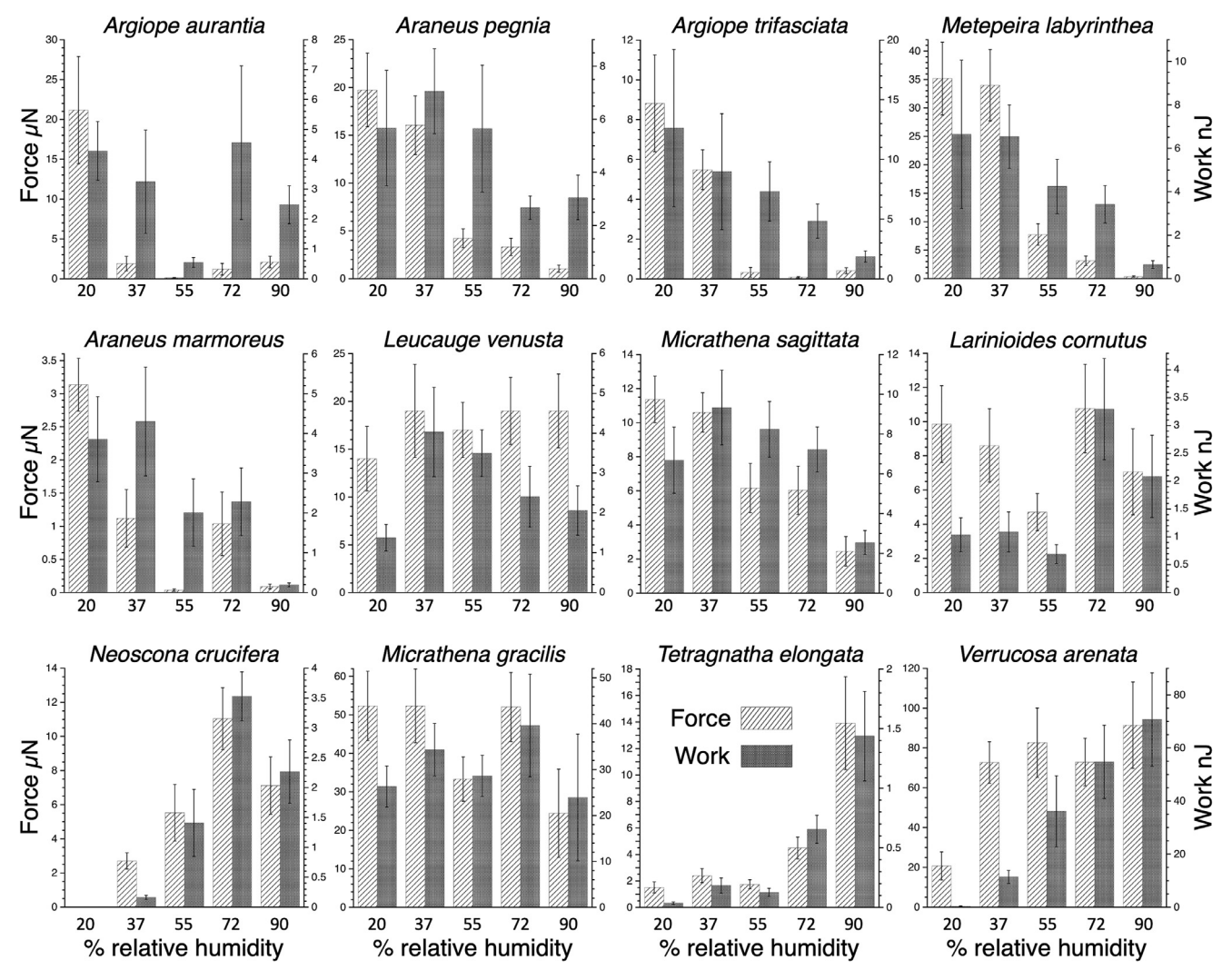


Fig. 9. Comparisons adhesive force (light shading) and the work of adhesion (dark shading) at test humidities. Error bars are  $\pm$  1 standard error.

humidity ranking scheme ( $R^2 = 0.73$ , Likelihood P = 0.0316) and the 4-humidity ranking scheme ( $R^2 = 1.00$ , Likelihood P = 0.0254).

We expanded this analysis to include four species (A. marmoreus, L. venusta, M. gracilis, and V. arenata) whose droplets exhibited maximum adhesive force at two humidities. To do this we first designated the humidity of the lower force peak as the humidity of a species' maximum force. When combined with the other eight species, this 12-species set exhibited a significant association between habitat humidity ranking and the rank of maximum adhesive force for both the 3-humidity ranking scheme ( $R^2 = 0.52$ , Likelihood P = 0.0361) and the 4-humidity ranking scheme ( $R^2 = 0.67$ , Likelihood P = 0.0402). We next designated the humidity of these four species' higher force peaks as the humidity of their maximum force and combined these with the other eight species. This 12species set also exhibited a significant association between habitat humidity ranking and the rank of maximum adhesive force for both the 3-humidity ranking scheme ( $R^2 = 0.57$ , Likelihood P = 0.0069) and the 4-humidity ranking scheme ( $R^2 = 0.69$ , Likelihood P = 0.0091).

### 3.6. Association of adhesive force and work of adhesion

There were general similarities between changes in adhesive force and the work of droplet extension to pull-off across test humidities (Fig. 9). However, because work is the sum of force

during a droplet's extension, work tended to change more uniformly across humidity than did force, as seen in *A. trifasciata*, *M. labyrinthea*, and *V. arenata*. In the seven species whose post 20% RH force peaked at a single humidity (*A. pegnia*, *A. trifasciata*, *M. labyrinthea*, *M. sagittata*, *N. crucifera*, *T. elongata*, and *V. arenata*), work peaked at the same humidity. In three other species (*A. marmoreus*, *L. cornutus*, and *M. gracilis*), work also peaked at the two humidities where maximum force was expressed. Only in *A. aurantia*, which expressed low force at all post 20% RH's, did adhesive force and the work of adhesion correspond poorly. The work of droplet extension peaked at a single post-20% RH in all species (Fig. 9). Contingency tests showed that this maximum work was correlated with both the 3- and 4-humidity rankings schemes ( $R^2 = 0.543$ , Likelihood P = 0.0111 and  $R^2 = 0.66$ , Likelihood P = 0.0140, respectively).

### 4. Discussion

A more highly integrated picture of glue droplet biomechanics emerges when adhesive contact is not restricted to core protein contact area. It appears that, upon contacting a surface, a droplet's low-viscosity aqueous layer [1,14] spreads rapidly, allowing its amorphous proteins [25] to establish a large area of adhesive contact. Solvated by LMMCs in the aqueous layer [15], the droplet's core protein combines with amorphous proteins in a manner that

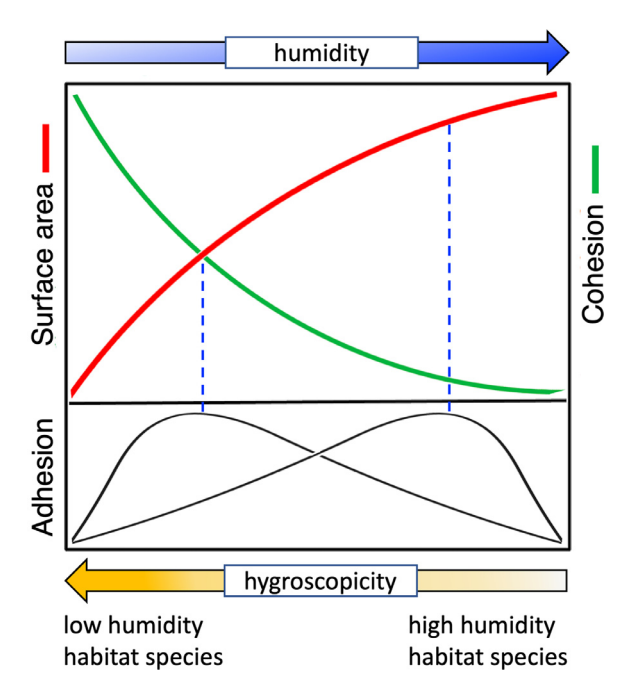


**Fig. 10.** A revised model of orb web spider glue droplet adhesion that accounts for observations presented in Figs. 4–6. In species that occupy low humidity habitats maximum adhesive force is registered when droplet area and protein cohesion lines intersect. Because species that occupy higher humidity habitats produce droplets with low hygroscopicity, higher humidity is required to soften their proteins and maximum adhesin is achieved at more divergent droplet area and protein elastic modulus values. This makes it possible for droplets of some species that are adapted to intermediate or variable humidity habitats to express high adhesive force at several humidities.

is not well understood to create a secure bond. As a droplet begins to extend and force on its core protein increases, LMMCs also withdraw interfacial water from the droplet footprint enhancing adhesion [28]. A granular region at the center of the protein core ensures that, as a droplet extends, its core protein filament remains firmly anchored to a thread's flagelliform fibers. Thus, just as a capture thread's glue droplets and flagelliform fibers are biomechanically integrated to form a suspension bridge that sums the adhesion of multiple droplets [9,11,12,37], the components of individual glue droplets appear to be functionally integrated to establish and transfer adhesive force. The earliest viscous capture threads may have consisted of flagelliform fibers covered by aqueous material. These threads would have been environmentally responsive, adhesive, and configured as a series of droplets. However, until core proteins were added, these simpler capture threads would not have generated as much adhesive force or summed this force as effectively as do the capture threads of modern orb weaving spiders.

The original model of glue droplet adhesion (Fig. 2) represents maximum adhesion as a single peak that occurs when area and cohesion converge, and implies that this peak is shifted to the left in species found in dry habitats and to the right in species found in humid habitats. Our results suggest a revised model (Fig. 10) in which the hygroscopic droplets of species that occupy dryer, exposed habitats (A. aurantia, A. pegnia, A. trifasciata, M. labyrinthea) and two intermediate humidity species (A. marmoreus and M. sagittata) conform to the original model by expressing maximum force at lower humidity near the point where the lines of rapidly increasing surface area and rapidly decreasing elastic modulus intersect. However, this model requires the addition of a second adhesive peak to explain the performance of droplets of one nocturnal species (N. crucifera) and two species found in high humidity habitats (T. elongate and V. arenata), which have less hygroscopic droplets. These species' droplets must become more fully hydrated

before their contact areas are great enough and their core proteins pliable enough to achieve peak adhesive force. The dual adhesion peaks of the revised model (Fig. 10) also explain the dual adhesion peaks of the intermediate humidity habitat species *L. venusta*, the nocturnal species *L. cornutus*, and the forest-dwelling species *M. gracilis*. The softening of a droplet's protein core as humidity increases has been attributed to an increase in the spacing of bonds that link protein molecules as additional water molecules are incorporated rather than to changes in the nature of these bonds [32]. It is also possible that increased water content increases the aqueous layer's pH, causing protein molecules to become more negatively charged and altering protein bonding or folding.

As hypothesized, both adhesive force and the work of extending a droplet to pull-off at humidities between 37% and 90% RH were associated with a species' foraging humidity. However, these observations also show that, when single glue droplet performance is considered, some species' core proteins can function well at several humidities or over a range of humidities, as seen in the forest edge species L. venusta, the nocturnal species L. cornutus, and the forest interior species M. gracilis and V. arenata (Fig. 9). This may not be surprising, as humidity can change over the course of a spider's foraging time. For example, individuals in our study population of *L. cornutus*, construct webs on supports of grain bins and edges of barns shortly after sunset, forage from the web's hub during the night, and, if their webs are not excessively damaged, continue to monitor them from a less conspicuous position at the web's perimeter during the following day. It is likely that during the night most prey are moths and during the day other insects. This is consistent with the adhesion of L. cornutus droplets, which exhibited a lesser force peak at 37% RH and a greater peak at 72% RH. Measurements of the adhesion of 12.58 mm spans of L. cornutus threads to glass and to insect surfaces with different setal textures also showed high adhesion at both 90% and 50% RH, although tests were not performed at other humidities [38].

Our study follows the convention of ranking the habitat humidity of diurnal species according to the humidity they typically experiences during late morning and afternoon hours and of nocturnal species, during evening and nighttime hours (Fig. 3), as inferred from prolonged humidity recordings in the habitats where these spiders were found (Fig. 4 in [2]). However, this does not mean that orb webs do not function at other humidities as mentioned for nocturnal species. Opell has observed *A. aurantia* and *A. trifasciata* feeding on grasshoppers in the early morning when humidity was very high. Thus, while natural selection may have tuned these species' capture threads to function optimally at low humidity, they continue to perform well enough at other humidities. The benefit of doing so may constrain the ability of selection to sharply tune the adhesion of these and other species' capture threads.

A previous study of *L. cornutus* thread adhesion uncoupled the effect of humidity on adhesive contact area and cohesion by adhering threads at one humidity and extending them at another humidity [14]. This showed that both insufficient and excessive droplet spreading led to pull-off before a droplet fully extended and was associated with lower work of thread peel. Threads registered more work when adhered at 50% RH and extended at 30% RH than when both adhered and extended at 50% RH. The lowest work was recorded when droplets were adhered at 70% RH and extended at 50% RH. This agrees with our adhesive force modeling (Fig. 7), which indicated that the pull-off force on a droplet increased when protein elastic modulus is increased relative to droplet contact area and decreased when area is increased relative to elastic modulus.

Our study identified large inter-humidity and inter-species differences in glue droplet properties (Fig. 3) and adhesive forces (Fig. 9). In this context, we believe that any shortcoming of our attempt to address the effect of humidity on flagelliform fiber elastic modulus did not obscure the broad picture that our results present of the response of orb web glue droplets to humidity. It would be difficult to explain how progressive changes in flagelliform fiber elastic modulus values across humidity could account for the contrasting and, in some species, oscillating patterns in droplet adhesive force and work that we observed.

#### 5. Conclusions

Our results support two hypotheses that have guided studies of orb web capture thread adhesion: 1. A glue droplet registers maximum adhesion when its viscosity is low enough to establish sufficient adhesive contact and its cohesion is high enough to transfer this force to the thread's axial fibers and 2. These optimal values are matched to a species' foraging humidity by droplet hygroscopicity. We found that a previous model of glue droplet adhesive performance was fundamentally valid, but in need of modification to accommodate some species that are found in intermediate and high humidity habitats. Because these species' droplets are less hygroscopic they do not register maximum adhesion until ambient humidity is sufficiently high to fully hydrated their aqueous material and protein cores. When incorporated into the previous model, this change also better explains the observation that some orb weavers found in intermediate and high and humidity habitats express high droplet adhesion at several humidities, with their droplets initially performing like those of low humidity species and later like those of high humidity species.

When viewing a flattened glue droplet, such as that shown in Fig. 1B, it is easy to infer that its dense core protein determines its adhesion. However, a droplet's aqueous layer plays a critical role in determining its performance by absorbing atmospheric moisture that hydrates all droplet components in a species-specific manner, by establishing initial adhesive contact, and by enhancing the core protein's adhesion. Our study further characterizes this synergy between a droplet's aqueous and core protein components, although a fuller picture of glue droplet biomechanics will require a better understanding of their molecular and structural integration.

## **Authors' contributions**

BDO developed the instrumentation used to characterize droplet features, collected thread samples and prepared droplets for extension, supervised and participated in droplet testing, established the workflow and formulas for determining adhesive material properties, conducted statistical analyses, prepared figures, and wrote the manuscript. HME assisted in setting up the file used to calculate material properties, measured droplet extension movies, and prepared summary tables of droplet features used in stress-strain curves. MLH measured the features of flattened glue droplets and computed droplet and core protein volumes.

## Funding

National Science Foundation grants IOS-1257719 and IOS-1755028 supported this study.

### **Declaration of Competing Interest**

The authors declare that they have no known competing financial interests that influenced the work reported in this paper.

### Acknowledgments

Sheree Andrews, Mary Clouse, Sarah Helweg, Kea Kiser, and Sarah Stellwagen assisted with droplet testing and measured suspended glue droplets. Sandra Correa-Garwhal characterized the elastic modulus of Araneus pegnia and Micrathena sagittata flagelliform fibers.

#### References

- G. Amarpuri, C. Zhang, C. Diaz, B.D. Opell, T.A. Blackledge, A. Dhinojwala, Spiders tune glue viscosity to maximize adhesion, ASC Nano 9 (2015) 11472–11478
- [2] B.D. Opell, H.M. Elmore, M.L. Hendricks, Humidity mediated performance and material properties of orb weaving spider adhesive droplets, Acta Biomater. 131 (2021) 440–451 Acta Biomater. 2021 Sep 1, doi:10.1016/j.actbio.2021.06. 017
- [3] W.S. Catalog, World spider catalog version 23.0, 2022. (Accessed March 4 2022).
- [4] C. Ewers-Saucedo, C.L. Owen, M. Pérez-Losada, J.T. Høeg, H. Glenner, B.K.K. Chan, K.A. Crandall, Towards a barnacle tree of life: integrating diverse phylogenetic efforts into a comprehensive hypothesis of thecostracan evolution, PeerJ 4 (2019) e1719, doi:10.7717/peerj.
- [5] WRMS, World registry of marine species, 2022. March 4, 2022.
- [6] G.H. Dickinson, I.E. Vega, K.J. Wahl, B. Orihuela, V. Beyley, E.N. Rodriguez, R.K. Everett, J. Bonaventura, D. Rittschof, Barnacle cement: a polymerization model based on evolutionary concepts, J. Exp. Biol. 212 (2009) 3499–3510.
- [7] K. Kamino, Molecular design of barnacle cement in comparison with those of mussel and tubeworm, J. Adhes. 86 (2010) 96–110.
- [8] N.A. Ayoub, K. Friend, T. Clarke, R. Baker, S. Correa-Garhwal, A. Crean, E. Dendev, D. Foster, L. Hoff, S.D. Kelly, W. Patterson, C.Y. Hayashi, B.D. Opell, Protein composition and associated material properties of cobweb spiders' gumfoot glue droplets, Integr. Comp. Biol. 14 (2021) 1459–1480.
- [9] B.D. Opell, M.L. Hendricks, The adhesive delivery system of viscous prey capture threads spin by orb-weaving spiders, J. Exp. Biol. 212 (2009) 3026–3034.
- [10] V. Sahni, T.A. Blackledge, A. Dhinojwala, Viscoelastic solids explain spider web stickiness, Nat. Commun. 1 (19) (2010) 1–4, doi:10.1038/ncomms1019.
- [11] Y. Guo, Y. Chang, H. Guo, W. Fang, Q. Li, H. Zhao, X. Feng, H. Gao, Synergistic adhesion mechanisms of spider capture silk, Interface 15 (2018) 20170894.
- [12] Y. Guo, H. Zhao, X. Feng, H. Gao, On the robustness of spider capture silk's adhesion, Extreme Mech. Lett. 29 (2019) 100477.
- [13] S. Kelly, B. Opell, H.M. Elmore, S. Correa-Garhwal, Correlated evolution between orb weaver glue droplets and supporting fibers maintains their distinct biomechanical roles in adhesion, J. Evol. Biol. 35 (2022) 879–890, doi:10.1111/jeb.14025
- [14] G. Amarpuri, C. Zhang, T.A. Blackledge, A. Dhinojwala, Adhesion modulation using glue droplet spreading in spider capture silk, J. R. Soc. Interface 14 (2017) 20170228
- [15] D. Jain, G. Amarpuri, J. Fitch, T.A. Blackledge, A. Dhinojwala, Role of hygroscopic low molecular mass compounds in responsive adhesion of spiders capture silk, Biomacromolecules 19 (2018) 3048–3057.
- [16] M.A. Townley, E.K. Tillinghast, Aggregate silk gland secretions of araneoid spiders, in: W. Nentwig (Ed.), Spider Ecophysiology, Springer-Verlag, New York, 2013, pp. 283–302.
- [17] B.D. Opell, C.M. Burba, P.D. Deva, M.H.Y. Kin, M.X. Rivas, H.M. Elmore, M.L. Hendricks, Linking properties of an orb weaving spider's capture thread glycoprotein adhesive and flagelliform fiber components to prey retention time, Ecol. Evol. 2019 (2019) 1–14.
- [18] B.D. Opell, D. Jain, A. Dhinojwala, T.A. Blackledge, Tuning orb spider glycoprotein glue performance to habitat humidity, J. Exp. Biol. 221 (2018) 1–12.
- [19] O. Choresh, B. Bayarmagnai, R.V. Lewis, Spider web glue: two proteins expressed from opposite strands of the same DNA sequence, Biomacromolecules 10 (2009) 2852–2856.
- [20] C. Hayashi, R. Lewis, Evidence from flagelliform silk cDNA for the structural basis of elasticity and modular nature of spider silks, J. Mol. Biol. 275 (1998) 773–784.
- [21] S.D. Stellwagen, R.L. Renberg, Toward spider glue: long read scaffolding for extreme length and repetitious silk family genes AgSp1 and AgSp2 with insights into functional adaptation, Genes Genom. Genet. 9 (2019) 1909–1919.
- [22] M.A. Collin, T.H. Clarke, N.A. Ayoub, C.Y. Hayashi, Evidence from multiple species that spider silk glue component ASG2 is a spidroin, Sci. Rep. 6 (2016) 21589.
- [23] J.A. Coddington, Spinneret silk spigot morphology: Evidence for the monophyly of orb-weaving spiders, Cyrtophorinae (Araneidae), and the group Theridiidae plus Nesticidae, J. Arachnol. 17 (1989) 71–96.
- [24] D. Edmonds, F. Vollrath, The contribution of atmospheric water vapour to the formation and efficiency of a spider's web, Proc. R. Soc. Lond. 248 (1992) 145–148.
- [25] G. Amarpuri, V. Chaurasia, D. Jain, T.A. Blackledge, A. Dhinojwala, Ubiquitous distribution of salts and proteins in spider glue enhances spider silk adhesion, Sci. Rep. 5 (9053) (2015) 1–7.
- [26] G.V. Guinea, M. Cerdeira, G.R. Plaza, M. Elices, J. Pérez-Rigueiro, Recovery in viscid line fibers, Biomacromolecules 11 (2010) 1174–1179.
- [27] V. Sahni, T. Miyoshi, K. Chen, D. Jain, S.J. Blamires, T.A. Blackledge, A. Dhinojwala, Direct solvation of glycoproteins by salts in spider silk glues enhances adhesion and helps to explain the evolution of modern spider orb webs, Biomacromolecules 15 (2014) 1225–1232.
- [28] S. Singla, G. Amarpuri, N. Dhopatkar, T.A. Blackledge, A. Dhinojwala, Hygroscopic compounds in spider aggregate glue remove interfacial water to maintain adhesion in humid conditions, Nat. Commun. 9 (2018) 1890.

- [29] B.D. Opell, M.I. Hendricks, The role of granules within viscous capture threads of orb-weaving spiders, J. Exp. Biol. 213 (2010) 339–346.
   [30] S.D. Kelly, B.D. Opell, L.L. Owens, Orb weaver glycoprotein is a smart biological
- [30] S.D. Kelly, B.D. Opell, L.L. Owens, Orb weaver glycoprotein is a smart biological material, capable of repeated adhesion cycles, Sci. Nat. 106 (10) (2019).
   [31] C. Riekela, M. Burghammerb, M. Rosenthalc, Skin-core morphology in spider
- [31] C. Riekela, M. Burghammerb, M. Rosenthalc, Skin-core morphology in spider flagelliform silk, Appl. Phys. Lett. 115 (2019) 123702.
  [32] V. Sahni, T.A. Blackledge, A. Dhinojwala, Changes in the adhesive properties of
- spider aggregate glue during the evolution of cobwebs, Sci. Rep. 1 (41) (2011) 1–8.
- [33] M. Czerner, L.S. Fellay, M.P. Suárez, P.M. Frontini, L.A. Fasce, Determination of elastic modulus of gelatin gels by indentation experiments, Procedia Mater. Sci. 8 (2015) 287–296.
- [34] B.D. Opell, A.M. Tran, S.E. Karinshak, Adhesive compatibility of cribellar and viscous prey capture threads and its implication for the evolution of orb-weaving spiders, J. Exp. Zool. 315 (2011) 376–384.

- [35] B.D. Opell, M.E. Clouse, S.F. Andrews, Elastic modulus and toughness of orb spider glycoprotein glue, PLoS One 13 (5) (2018) e0196972 21 pages.
- [36] B.D. Opell, M.E. Clouse, S.F. Andrews, Elastic modulus and toughness of orb spider glycoprotein glue, PLoS One 13 (5) (2018) e0196972 21 pages.
- [37] S.D. Kelly, B.D. Opell, S.M. Correa-Garwhal, Correlated evolution between orb weaver glue droplets and supporting fibres maintains their distinct biomechancal roles in adhesion, J. Evol. Biol. 35 (2022) 879–890.
- [38] A.M. Alicea-Serrano, A. Onyak, A. Dhinojwala, T.A. Blackledge, Robust performance of spider viscid silk on hairy and smooth insect substrates, Integr. Comp. Biol. 61 (4) (2021) 1432–1439.
- Comp. Biol. 61 (4) (2021) 1432–1439.
  [39] A. Sensenig, I. Agnarsson, T.A. Blackledge, Behavioral and biomaterial coevolution in spider orb webs, J. Evol. Biol. 23 (2010) 1839–1856.